

Recurrence of optical squeezing: witness of nonclassicality in optomechanics

Yue Ma¹, Federico Armata¹, Kiran E. Khosla¹, and M. S. Kim^{1,2}

¹*QOLS, Blackett Laboratory, Imperial College London, London SW7 2AZ, United Kingdom*

²*Korea Institute of Advanced Study, Seoul 02455, South Korea*

Witnessing nonclassicalities in the mechanical motion of mesoscopic objects is one of the important goals in optomechanics. Here, the dynamics of micro-mechanical elements can be read out by high precision measurements on the optical field. In this context, we study how nonclassicality of a mechanical movable mirror can be revealed by measuring the optical field variance alone. By developing classical and semiclassical descriptions of the system, without requiring quantization of the mirror, we recover either squeezing of the optical field or revivals in the field variance. We identify the recurrence of squeezing in the optical field as a genuine witness of nonclassicality of mechanical motion.

Introduction — Cavity optomechanics studies the interaction between an electromagnetic cavity mode and a movable mechanical element. These systems are proposed as candidates to have significant impact on both foundations of physics [1] and practical applications [2]. The field has the potential to lead to understanding of a large number of deep questions, including decoherence mechanisms [3, 4] and gravitational effects in quantum mechanics [5–8]. It also promises quantum enhanced metrology with high-precision optomechanical sensing including force [9], magnetic field [10], acceleration [11], radio frequency radiation [12].

The optomechanical interaction causes the optical field to become correlated with the motion of the mechanical oscillator [13–15]. Measurement on the optical field can therefore reveal properties of the mechanical oscillator, including its nonclassicality [2, 16]. It is known that, the entanglement between two optical modes interacting sequentially with a mechanical oscillator unambiguously proves the nonclassicality of the mechanical oscillator [17, 18]. However, due to the difficulty in implementing a Bell test of a continuous-variable optical field, it is desirable to come up with other witnesses of mechanical nonclassicality. In this direction, we consider optomechanical squeezing [19, 20] which has been observed in several experimental setups [21–23]. It is natural to ask whether its observation can prove the nonclassicality of the mechanical oscillator.

In this Letter we study what nontrivial behaviors of field variance can act as a witness for mechanical nonclassicality. We propose several classical and semiclassical descriptions of the optomechanical interaction without quantizing the oscillator. By comparing the time evolution of the field variance with that predicted in the standard quantum mechanical description, we find that without quantizing the mechanical motion, we can still get squeezing of the field, but not the recurrence of squeezing, which can thereby act as a witness for oscillator quantization. We also discuss the effect of cavity loss and the measurement of the output cavity field.

Quantum and classical descriptions — We consider the standard optomechanical system consisting of a Fabry-Pérot cavity with a movable mirror, shown in Fig. 1(a), with the equilibrium frequency of the oscillator (field)

given by ω (Ω). The Hamiltonian in the frame rotating with the optical frequency Ω is given by [24, 25]

$$\hat{H}/\hbar = \omega \hat{b}^\dagger \hat{b} - \frac{g_0}{\sqrt{2}} \hat{a}^\dagger \hat{a} (\hat{b}^\dagger + \hat{b}), \quad (1)$$

where \hat{a} (\hat{b}) is the optical (mechanical) annihilation operator and $g_0/\sqrt{2}$ is the single-photon optomechanical coupling strength. This Hamiltonian can be understood as (an oscillator-mediated) intensity-dependent phase shift of the optical field [26].

For the quantum description, we consider the initial state of the intracavity field in a coherent state $|\alpha\rangle_L$ with real α , and the mechanical oscillator in a vacuum state (for the generalization to the initial thermal states see [27]). The Hamiltonian in Eq. (1) can be directly mapped into a classical Hamiltonian, with classical canonical field (oscillator) variables $\alpha_L, \alpha_L^*(x, p)$. Classical uncertainty in the field (oscillator) is represented by a classical probability distribution of α_L (x and p) over phase space, representing the ignorance of the exact state of the system [28]. In this case the evolution can be understood in terms of a Fokker-Planck equation for the joint optomechanical probability distribution or by deterministic evolution of variables using stochastic initial conditions drawn from a probability distribution matching the initial quantum state. For the optomechanical Hamiltonian, the latter is more efficient and is used in this work. Specifically, we choose the initial amplitude of the field $\alpha_L(0) = \alpha + \delta$, where α is the amplitude of the coherent state $|\alpha\rangle_L$, and δ is a complex zero mean Gaussian random variable with covariance matrix $\text{diag}(1/2, 1/2)$, thereby classically simulating the vacuum noise. The initial position and momentum of the mechanical oscillator satisfy the Maxwell-Boltzmann distribution such that the initial classical variance matches the quantum ground state variance.

The time evolution of the field in the quantum [29] and classical descriptions [27] are calculated to be

$$\hat{a}(t) = e^{iA(t)/2} e^{k((1-e^{-i\omega t})\hat{b} - (1-e^{i\omega t})\hat{b}^\dagger)} e^{iA(t)\hat{a}^\dagger \hat{a}} \hat{a} \quad (2a)$$

$$\alpha_L(t) = e^{i\sqrt{2}k(x(0)\sin\omega t + p(0)(1-\cos\omega t))} e^{iA(t)|\alpha_L(0)|^2} \alpha_L(0) \quad (2b)$$

where we have defined the non-negative function $A(t) = 2k^2(\omega t - \sin \omega t)$, with $k = g_0/(\sqrt{2}\omega)$. For the classical equation of motion, we have solved classical Hamilton's equations, which depicts a deterministic time evolution of a closed system for a given realization of δ , $x(0)$ and $p(0)$. The random initial conditions can simply be integrated out using the appropriate probability density kernels.

To see the optical squeezing, we calculate the time evolution of the quadrature variances using the solutions in Eqs. (2). We define the θ -dependent quadrature operator as $\hat{X}_\theta(t) = \hat{a}(t)e^{-i\theta} + \hat{a}^\dagger(t)e^{i\theta}$, and the corresponding variance as $\text{Var}_\theta(t) = \langle \hat{X}_\theta^2(t) \rangle - \langle \hat{X}_\theta(t) \rangle^2$, with a similar expression for the classical field (replacing the quantum expectation value with a classical ensemble average). Squeezing is defined based on the minimum of variance taken over all quadrature angles, $\text{Var}(t) \equiv \min_\theta \{\text{Var}_\theta(t)\}$, as in general the maximally squeezed quadrature is expected to be time dependent. If $\text{Var}(t) < 1$, then the field is squeezed at time t , with $\text{Var}_\theta(0) = 1$ (the initial condition) serving as the reference level for both quantum and classical “squeezing”. One is interested in how the variance evolves in time, and whether it is possible to distinguish classical and quantum evolution using the variance alone.

The time evolution of $\text{Var}(t)$ for the quantum and classical descriptions are shown in the blue solid and red dotted lines in Fig. 1(b) respectively (see the analytical expressions in [27]). For simplicity we only plot the non-trivial parts where the variances in different descriptions can be distinguished. Here we choose a coherent state $\alpha = 20$, with strong optomechanical interaction $k = 0.01$, similar parameters predicted in the high cooperativity regime of thin-film superfluid [30] (for a choice of other parameter values, see [27]). The quantum and classical variances are nearly identical during the initial evolution, as long as $\alpha^2 \gg 1$ and $k^2 \ll 1$, which is the case in most of the optomechanical experiments. For both quantum and classical evolution, the field is squeezed for the first few mechanical periods, followed by a rapid increase in the variance to a value $2\alpha^2 + 1$. The difference between the two descriptions appears at the first revival after a long interaction time. After approximately $t = \tau/4k^2$, where $\tau = 2\pi/\omega$ is the mechanical period, there is a quantum revival where variance rapidly returns to $\gtrsim 1$ for several mechanical periods before again stabilising at $2\alpha^2 + 1$. There is another qualitatively different revival after a second interval of $\approx \tau/4k^2$. In this second revival, the quantum variance again rapidly decreases, however this time squeezing reappears. The two quantum revivals are repeated periodically.

In contrast, the classical variance stabilises to $2\alpha^2 + 1$ after the first several oscillations and never exhibits revivals [31]. The increase to and stabilization at $2\alpha^2 + 1$ have different reasons for the two descriptions. Quantum mechanically it arises from a phase mismatch between different Fock state components making up the initial coherent state. The discreteness of energy levels leads to periodical synchronization of the phases. At some

times, partial synchronization results in half revival of the variance. The field is in a cat-state superposition of $|\alpha\rangle + |-\alpha\rangle$, hence no squeezing is possible. This corresponds to the first type of quantum revival as discussed above. At other times, fully synchronization results in full revival of the variance. The field returns to a full coherent state $|\alpha\rangle$, leading to the observed squeezing as shown in the second type of quantum revival. Classically, each point in phase space rotates at a different, radial-dependent rate, thereby smearing the initial phase space distribution around a circle of radius $\approx \alpha$. The variance $2\alpha^2 + 1$ represents a mixture over a continuum of phase space rotations with no possibility of constructive interference, hence the stabilization to $2\alpha^2 + 1$.

The existence of quantum revivals is a direct result of the discrete energy levels of the field, a typical example of which is the collapse and revival of atomic excitation in the Jaynes-Cummings model [32]. The detection of quantum revivals can distinguish quantum and classical descriptions so far. The minimum condition to observe the first revival of squeezing is $g_0^2/(\omega\kappa) > 1$, where κ is the dissipation rate of the cavity field. This is known as the single-photon blockade condition [2]. It is the requirement that the field has not leaked out from the cavity by the time of the revivals, and is a stronger requirement than strong single photon cooperativity, $\mathcal{C}_0 = 2g_0^2/(\kappa\gamma) > 1$, with γ the mechanical dissipation rate. Single photon blockade regime has not yet been achieved in optomechanical experiments with the possible exception of ultracold atoms [33, 34].

We have seen both quantum and classical descriptions give the same initial squeezing, with revivals at later times being a clear signature of quantization. However it is not clear which phenomenon is a result of quantization of the oscillator itself. This will be clarified in the following sections where we consider several semiclassical models for the optomechanical system.

Mean field approximation — The quantum nature of the electromagnetic field has already been demonstrated experimentally. As a result, the fully classical description is not expected to be a physical description of any experimental device. Here we consider several semiclassical models with quantum field and classical oscillator. Fundamentally, a quantum mode is incompatible with a classical mode, and a unique, unambiguous semiclassical description does not exist, requiring extra assumptions for a self-consistent theory [35–38]. In this section, we consider the mean field approximation consisting of a quantum interaction Hamiltonian $\hat{H}_L = -g_0x(t)\hat{a}^\dagger\hat{a}$ for the quantized field, and a classical Hamiltonian $H_M = \frac{1}{2}\omega(x^2(t) + p^2(t)) - g_0Ix(t)$ for the classical mechanical oscillator. The dimensionless intensity I is time-independent as $[\hat{H}_L, \hat{a}^\dagger\hat{a}] = 0$.

The quantity I can be interpreted in several different ways depending on the level of the field’s “quantumness” the classical oscillator can see. Here we consider three reasonable possibilities for I . Firstly, the oscillator sees only the mean field, hence I is given by the standard

mean field $I = \langle \alpha | \hat{a}^\dagger \hat{a} | \alpha \rangle$ approximation. Secondly, the oscillator sees the energy quanta of the field with I given by a random number. While the oscillator sees individual quanta, it cannot see different quanta in superposition, and hence evolves as though there were a mixture of Fock state inside the cavity. In this case I is a Poisson random variable with mean and variance α^2 , coinciding with the photon number distribution for a coherent state. Thirdly, the oscillator can detect fluctuations in the field intensity, but it cannot tell the discreteness of the energy. I is thus well approximated by a Gaussian distribution with its mean and variance α^2 , where the approximation holds to the extent that the Poisson distribution of I appears Gaussian when $\alpha^2 \gg 1$.

For each case $\text{Var}(t)$ is plotted in Fig. 1(b), where the grey dot-dashed, orange dashed and green solid lines correspond to constant, Poisson and Gaussian I , respectively. Constant I results in a small periodical variation above the initial value 1 at the period of the mechanical oscillation due to the stochastic initial condition of the oscillator. A Poisson distributed I does not exhibit squeezing, but successfully reproduces the periodical revivals at the same times as the quantum description. Although quantum revivals are believed to be signatures of the quantumness of a system, here the classical nature of the mechanical oscillator does not preclude quantum revivals of the field. Quantum revivals are a result of field quantization, which guarantees that I only takes integer values. It is not related to whether the oscillator is quantized by representing x and p with \hat{b} and \hat{b}^\dagger . A Gaussian distributed I , although acting as a continuous approximation of Poisson distribution, does not leave the field variance similar to the Poissonian case. The difference lies in that, there is no revival for a Gaussian I . The continuous approximation smears out the discreteness of the field intensity which is a crucial factor leading to the quantum revivals.

In fact, the quantum interaction Hamiltonian $\hat{H}_L = -g_0 x(t) \hat{a}^\dagger \hat{a}$ only induces a frequency modulation of the optical field, which cannot reduce the field variance. This is true for any classical $x(t)$ regardless of the dependence of $x(t)$ on $\rho(t)$. Consider the evolution of the density matrix in a small time step δt , $\rho(t + \delta t) = \exp[ig_0 \delta t x(t) \hat{a}^\dagger \hat{a}] \rho(t) \exp[-ig_0 \delta t x(t) \hat{a}^\dagger \hat{a}]$. If $x(t)$ does not contain any randomness, the unitary induces a rotation in the optical phase space, $\hat{a} \rightarrow \exp[ig_0 \delta t x(t)] \hat{a}$, which cannot change the minimal variance. If $x(t)$ does contain classical randomness, the evolution is a convex mixture of rotations, with $\rho(t + \delta t) = \sum_j P_j \rho_j(t + \delta t)$, where P_j is the probability for $x(t)$ to take value x_j , and $\rho_j(t + \delta t)$ is the evolution of the state based on x_j . The concavity of the variance for two probability distributions P and Q , $\text{Var}[\lambda P + (1 - \lambda)Q] \geq \lambda \text{Var}(P) + (1 - \lambda) \text{Var}(Q)$ with $\lambda \in [0, 1]$, ensures that minimal variance must increase, therefore squeezing for the mean field semiclassical dynamics is impossible.

The impossibility to give squeezing in the mean field semiclassical description lies in the fact that back action

from the oscillator to the field is not correctly captured. Quantum and classical descriptions discussed in the previous section, in contrast, model the back action via the correlation of amplitude and phase noise of the field mediated by the oscillator, thus predicting squeezing. In order to include the back action of the classical oscillator on the quantum field, we introduce a semiclassical measurement model in the next section, where the oscillator evolves based on the instantaneous field intensity it sees and in turn collapses the field state continuously.

Semiclassical measurement model — The mean field assumption does not capture the interpretation of quantum fluctuations in the optomechanical system. Here we introduce a description based on the semiclassical model discussed in Ref. [39]. The classical oscillator effectively measures the intensity of the quantum field, thereby collapsing its wave function [40, 41]. This collapse was missing in the previous semiclassical models where the oscillator saw a discrete intensity while the field was allowed to remain in a coherent state. During an infinitesimal time step, the mechanical oscillator gains an infinitesimal amount of information about the instantaneous intensity of the field, and its position and momentum evolve consequently. In turn, the field evolves taking into account both the new position of the mechanical oscillator, and the fact that some classical information has been extracted by the oscillator (i.e. quantum collapse).

The equations of motion are [40–42]

$$d\rho = ig_0 x dt [\hat{a}^\dagger \hat{a}, \rho] - \Gamma dt [\hat{a}^\dagger \hat{a}, [\hat{a}^\dagger \hat{a}, \rho]] + \sqrt{2\Gamma} \left(\{\hat{a}^\dagger \hat{a}, \rho\} - 2\text{Tr}(\rho \hat{a}^\dagger \hat{a}) \rho \right) dW, \quad (3a)$$

$$dx = \omega p dt, \quad (3b)$$

$$dp = -\omega x dt + g_0 \text{Tr}(\rho \hat{a}^\dagger \hat{a}) dt + \frac{g_0}{2\sqrt{2\Gamma}} dW, \quad (3c)$$

where Γ characterises the rate at which classical information is gained by the oscillator, and dW is the Wiener differential – a zero mean Gaussian random variable with variance dt . Each term in Eqs. (3a)–(3c) can be physically understood. The double commutator describes dephasing of the quantum field, and is stabilised around a Fock state, where exactly which Fock state depends on one specific realisation of dW . The classical oscillator sees the effect of the field through the measurement of the intensity of the field, which depends on both the average intensity and the classical fluctuations, thereby introducing noise correlations between the field and the oscillator.

Eqs. (3a)–(3c) are solved numerically, and the resulting field variances as a function of time are shown in Fig. 1(c). For numerical reasons, we set $\alpha = 2$ and $k = 0.1$. We keep the product αk the same as that in the quantum description, where this product determines the maximum amount of squeezing. For the mechanical oscillator, we simulate both the case with $x(0) = p(0) = 0$ (red line), and the case with $x(0)$ and $p(0)$ satisfying a Maxwell-Boltzmann distribution where their variances match the

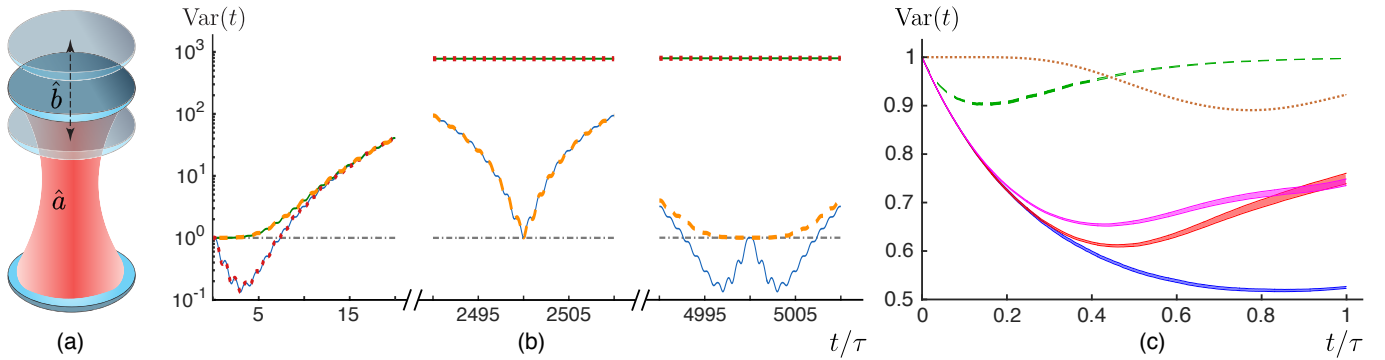


FIG. 1. (a) A Fabry-Pérot cavity with one movable ending mirror described as a harmonic oscillator. (b) Field variance as a function of time for quantum (blue solid line) and classical (red dotted line) description, mean field semiclassical descriptions with constant I (grey dot-dashed line), Poisson random I (orange dashed line), and Gaussian random I (green solid line). All plots use $\alpha = 20$, $k = 0.01$. (c) Field variance as a function of time for the semiclassical measurement model with $k = 0$ (blue line), $k = 0.1$, $x(0) = 0$, $p(0) = 0$ (red line), $k = 0.1$, $x(0)$ and $p(0)$ as classical random variables simulating the zero-point-fluctuation (pink line). All curves use $\alpha = 2$, $\Gamma = 0.01\omega$. For comparison, the effect of cavity dissipation is shown for the semiclassical model (green dashed line) with photon dissipation rate $\kappa = \omega$, and the quantum model (brown dotted line) with $\kappa = 0.3\omega$. The width of the line for numerical solutions represents mean \pm standard deviation.

quantum zero-point-fluctuation (pink line). The strength of the continuous measurement Γ is theoretically a free parameter, but here it is chosen as $\Gamma = 0.01\omega$ such that both the optomechanical interaction and the continuous measurement play important roles. Squeezing of the field appears in both cases. The existence of initial thermal noise shows negligible influence on the field variance at the start of the evolution. In fact, the field is squeezed in every noise realisation, before taking the ensemble average.

In this model, squeezing arises from the transient evolution from a coherent state to a specific Fock state, which is induced by the effective photon number measurement Eq. (3a). The realization of $dW(t)$ continuously forces the field to evolve into a random Fock state. Once a specific Fock state is preferred, the probability for the field to take other possible Fock states decreases, thus reducing the uncertainty in the number basis. This number squeezed state can be well approximated by a quadrature squeezed state for a small amount of number squeezing. Note the squeezing only appears in the early stage of the time evolution, when the number squeezed \sim quadrature squeezed approximation is valid. Eventually the state will approach a $dW(t)$ -dependent Fock state, and averaging over all realizations of $dW(t)$ results in an incoherent mixture of Fock states [43].

In this model the squeezing is a result of the weak measurement and not the unitary dynamics of the mechanical oscillator. As such, the amount of squeezing is always smaller than the case when, the field intensity is continuously measured by an apparatus without dynamics, which is shown as the blue line in Fig. 1(c) with $k = 0$. This is because the unitary evolution of the oscillator induces a convex mixture of rotations of the optical field in phase space, as discussed in the mean field semiclassical model. Without this convex mixture of rotations (i.e.

$k = 0$), the maximum amount of squeezing is always at $\theta = 0$ for a real α .

Open cavity dynamics — So far we have considered only the intracavity field, and not commented on how photons exit the cavity to be detected. For our parameters intracavity squeezing appears over one mechanical period τ . Using the cavity input-output relations [44], and considering a highly dissipative cavity, the output field is dominated by the intracavity squeezed field. The green dashed line in Fig. 1(c) simulates the variance of the intracavity field in the presence of photon dissipation with rate $\kappa = \omega$, where cavity decay is simulated with the standard quantum optical Lindblad term in the master equation [45]. The squeezing is reduced but does not completely vanish. The squeezing in the output field may be observed using time-binned homodyne detection [46], and choosing the temporal profile of the local oscillator to capture only the squeezed part of the outgoing field [47]. However, this requirement of large dissipation implies quantum revivals cannot be observed in this parameter regime.

For comparison, we plot the field variance predicted by a fully quantum description in the presence of dissipation $\kappa = 0.3\omega$ (Fig. 1(c), brown dotted line). Cavity loss has a stronger effect as the squeezing is reduced to a level similar to that of the semiclassical measurement model with a larger dissipation rate. It is also clear that maximal squeezing appears at a later time for the quantum description.

Conclusion — We have proposed a classical description and several semiclassical descriptions for an optomechanical system without quantizing the mechanical oscillator, and studied how the time evolutions of the optical field variance differ from that predicted by the standard quantum mechanical description. Even if the oscillator is not quantized, as long as the backaction onto the field is cap-

tured, the field shows squeezing at the beginning of the evolution. Likewise, quantum revivals in the field variance do not indicate quantization of the oscillator either, as the semiclassical description with classical oscillator able to detect the granularity of the optical intensity predicts quantum revivals. Our study puts a clear boundary on the possibility of using field variance to deduce the nonclassicality of mechanical oscillator. The boundary turns out to be the single-photon blockade condition. Once it is satisfied, the revival of optical squeezing rules out the descriptions discussed here based on a classical

oscillator, thus being a witness of mechanical nonclassicality. The classical and semiclassical descriptions introduced here can possibly be applied to the analysis of other potential witnesses of nonclassicality as well.

Acknowledgements — MSK and KK acknowledge the Leverhulme Trust [Project RPG-2014-055] and the Royal Society. FA and MSK acknowledge the Marie Curie Actions of the EU's 7th Framework Programme under REA [grant number 317232]. YM acknowledges the Imperial College President's PhD Scholarship.

-
- [1] I. Pikovski, M. R. Vanner, M. Aspelmeyer, M. S. Kim, and Č. Brukner, *Nat. Phys.* **8**, 393 (2012).
 - [2] M. Aspelmeyer, T. J. Kippenberg, and F. Marquardt, *Rev. Mod. Phys.* **86**, 1391 (2014).
 - [3] R. Penrose, *Phil. Trans. R. Soc. A* **356**, 1927 (1998).
 - [4] W. Marshall, C. Simon, R. Penrose, and D. Bouwmeester, *Phys. Rev. Lett.* **91**, 130401 (2003).
 - [5] R. Penrose, *Gen. Rel. Gravit.* **28**, 581 (1996).
 - [6] L. Diósi, *Phys. Rev. A* **40**, 1165 (1989).
 - [7] J. Schmöle, M. Dragosits, H. Hepach, and M. Aspelmeyer, *Class. Quantum Grav.* **33**, 125031 (2016).
 - [8] A. Plato, C. Hughes, and M. S. Kim, *Contemp. Phys.* **57**, 477 (2016).
 - [9] E. Gavartin, P. Verlot, and T. J. Kippenberg, *Nat. Nanotechnol.* **7**, 509 (2012).
 - [10] S. Forstner, S. Prams, J. Knittel, E. Van Ooijen, J. Swaim, G. Harris, A. Szorkovszky, W. Bowen, and H. Rubinsztein-Dunlop, *Phys. Rev. Lett.* **108**, 120801 (2012).
 - [11] A. G. Krause, M. Winger, T. D. Blasius, Q. Lin, and O. Painter, *Nat. Photonics* **6**, 768 (2012).
 - [12] T. Bağcı, A. Simonsen, S. Schmid, L. G. Villanueva, E. Zeuthen, J. Appel, J. M. Taylor, A. Sørensen, K. Usami, A. Schliesser, *et al.*, *Nature* **507**, 81 (2014).
 - [13] M. R. Vanner, I. Pikovski, G. D. Cole, M. S. Kim, Č. Brukner, K. Hammerer, G. J. Milburn, and M. Aspelmeyer, *Proc. Natl. Acad. Sci.* **108**, 16182 (2011).
 - [14] M. R. Vanner, I. Pikovski, and M. S. Kim, *Ann. Phys. (Berl.)* **527**, 15 (2015).
 - [15] L. Latmiral, F. Armata, M. G. Genoni, I. Pikovski, and M. S. Kim, *Phys. Rev. A* **93**, 052306 (2016).
 - [16] F. Armata, L. Latmiral, I. Pikovski, M. R. Vanner, Č. Brukner, and M. S. Kim, *Phys. Rev. A* **93**, 063862 (2016).
 - [17] V. C. Vivoli, T. Barnea, C. Galland, and N. Sangouard, *Phys. Rev. Lett.* **116**, 070405 (2016).
 - [18] I. Marinkovic, A. Wallucks, R. Riedinger, S. Hong, M. Aspelmeyer, and S. Gröblacher, *arXiv preprint arXiv:1806.10615* (2018).
 - [19] C. Fabre, M. Pinard, S. Bourzeix, A. Heidmann, E. Giacobino, and S. Reynaud, *Phys. Rev. A* **49**, 1337 (1994).
 - [20] S. Mancini and P. Tombesi, *Phys. Rev. A* **49**, 4055 (1994).
 - [21] D. W. Brooks, T. Botter, S. Schreppler, T. P. Purdy, N. Brahms, and D. M. Stamper-Kurn, *Nature* **488**, 476 (2012).
 - [22] T. Purdy, P.-L. Yu, R. Peterson, N. Kampel, and C. Regal, *Phys. Rev. X* **3**, 031012 (2013).
 - [23] A. H. Safavi-Naeini, S. Gröblacher, J. T. Hill, J. Chan, M. Aspelmeyer, and O. Painter, *Nature* **500**, 185 (2013).
 - [24] A. Pace, M. Collett, and D. Walls, *Phys. Rev. A* **47**, 3173 (1993).
 - [25] C. Law, *Phys. Rev. A* **51**, 2537 (1995).
 - [26] D. James and J. Jerke, *Can. J. Phys.* **85**, 625 (2007).
 - [27] See supplementary material.
 - [28] T. Marshall and E. Santos, *Found. Phys.* **18**, 185 (1988).
 - [29] S. Mancini, V. Man'ko, and P. Tombesi, *Phys. Rev. A* **55**, 3042 (1997).
 - [30] C. G. Baker, G. I. Harris, D. L. McAuslan, Y. Sachkou, X. He, and W. P. Bowen, *New J. Phys.* **18**, 123025 (2016).
 - [31] G. Milburn, *Phys. Rev. A* **33**, 674 (1986).
 - [32] J. H. Eberly, N. Narozhny, and J. Sanchez-Mondragon, *Phys. Rev. Lett.* **44**, 1323 (1980).
 - [33] K. W. Murch, K. L. Moore, S. Gupta, and D. M. Stamper-Kurn, *Nat. Phys.* **4**, 561 (2008).
 - [34] F. Brennecke, S. Ritter, T. Donner, and T. Esslinger, *Science* **322**, 235 (2008).
 - [35] K. Eppley and E. Hannah, *Found. Phys.* **7**, 51 (1977).
 - [36] L. Diósi, N. Gisin, and W. T. Strunz, *Phys. Rev. A* **61**, 022108 (2000).
 - [37] S. L. Adler, *Nucl. Phys. B* **415**, 195 (1994).
 - [38] H.-T. Elze, *Phys. Rev. A* **85**, 052109 (2012).
 - [39] L. Diósi, *Phys. Lett. A* **129**, 419 (1988).
 - [40] K. Jacobs and D. A. Steck, *Contemp. Phys.* **47**, 279 (2006).
 - [41] L. Diósi and J. J. Halliwell, *Phys. Rev. Lett.* **81**, 2846 (1998).
 - [42] H. M. Wiseman and G. J. Milburn, *Quantum measurement and control* (Cambridge university press, 2009).
 - [43] M. Fox, *Quantum optics: an introduction*, Vol. 15 (OUP Oxford, 2006).
 - [44] M. Collett and C. Gardiner, *Phys. Rev. A* **30**, 1386 (1984).
 - [45] C. Gardiner and P. Zoller, *Quantum noise: a handbook of Markovian and non-Markovian quantum stochastic methods with applications to quantum optics*, Vol. 56 (Springer Science & Business Media, 2004).
 - [46] D. Smithey, M. Beck, M. G. Raymer, and A. Faridani, *Phys. Rev. Lett.* **70**, 1244 (1993).
 - [47] T. Opatrny, D.-G. Welsch, and W. Vogel, *Phys. Rev. A* **55**, 1416 (1997).

Supplementary material: Optical field variance as a witness of mechanical nonclassicality in optomechanics

Yue Ma¹, Federico Armata¹, Kiran E. Khosla¹, and M. S. Kim^{1,2}

¹*QOLS, Blackett Laboratory, Imperial College London, London SW7 2AZ, United Kingdom*

²*Korea Institute of Advanced Study, Seoul 02455, South Korea*

(Dated: May 20, 2022)

I. ANALYTICAL EXPRESSIONS OF VARIANCE IN THE QUANTUM, CLASSICAL AND SEMICLASSICAL MEAN FIELD DESCRIPTIONS

The full expression of the field variance in the quantum description is given by

$$\begin{aligned} \text{Var}_\theta^{(q)}(t) &= \langle \hat{X}_\theta^2(t) \rangle - \langle \hat{X}_\theta(t) \rangle^2 = \\ &2\alpha^2 e^{-\alpha^2(1-\cos 2A(t))} e^{-2B(t)} \cos(2A(t) + \alpha^2 \sin 2A(t) - 2\theta) \\ &- 2\alpha^2 e^{-2\alpha^2(1-\cos A(t))} e^{-B(t)} \cos(A(t) + 2\alpha^2 \sin A(t) - 2\theta) \\ &+ 2\alpha^2 \left(1 - e^{-2\alpha^2(1-\cos A(t))} e^{-B(t)}\right) + 1. \end{aligned} \quad (1)$$

Here we consider the initial state of the intracavity field to be a coherent state $|\alpha\rangle_L$, and the mechanical oscillator to be a thermal state $\hat{\rho}_{\text{th}} = \sum_{n=0}^{\infty} p_n |n\rangle\langle n|$ at temperature T , where $p_n = \tilde{n}_{\text{th}}^n / (\tilde{n}_{\text{th}} + 1)^{n+1}$ with $\tilde{n}_{\text{th}} = 1/(\exp(\hbar\omega/k_B T) - 1)$, and $|n\rangle$ a Fock state. The

functions are defined as $A(t) = 2k^2(\omega t - \sin \omega t)$ and $B(t) = 2k^2(2\tilde{n}_{\text{th}} + 1)(1 - \cos \omega t)$.

To express the full expression of the field variance as a function of time in the classical description, we first define several functions to simplify the notation:

$$d_1(k, \omega, t) = 2A^2(t)/(1 + A^2(t)), \quad (2a)$$

$$d_2(k, \omega, t) = 2A^2(t)/(4 + A^2(t)), \quad (2b)$$

$$d_3(k, \omega, t) = 16/(4 + A^2(t))^2, \quad (2c)$$

$$c_1(k, \omega, t) = (1 - 3A^2(t))/(1 + A^2(t))^3, \quad (2d)$$

$$c_2(k, \omega, t) = (256 - 384A^2(t) + 16A^4(t))/(4 + A^2(t))^4, \quad (2e)$$

$$s_1(k, \omega, t) = (3A(t) - A^3(t))/(1 + A^2(t))^3, \quad (2f)$$

$$s_2(k, \omega, t) = (512A(t) - 128A^3(t))/(4 + A^2(t))^4, \quad (2g)$$

$$\phi_1(k, \omega, t) = 2A(t)/(1 + A^2(t)), \quad (2h)$$

$$\phi_2(k, \omega, t) = 4A(t)/(4 + A^2(t)). \quad (2i)$$

The variance in the classical picture is then

$$\begin{aligned} \text{Var}_\theta^{(c)}(t) &= 2\alpha^2 e^{-\alpha^2 d_1(k, \omega, t)} e^{-2C(t)} \left(c_1(k, \omega, t) \cos(\alpha^2 \phi_1(k, \omega, t) - 2\theta) - s_1(k, \omega, t) \sin(\alpha^2 \phi_1(k, \omega, t) - 2\theta) \right) \\ &- 2\alpha^2 e^{-2\alpha^2 d_2(k, \omega, t)} e^{-C(t)} \left(c_2(k, \omega, t) \cos(2\alpha^2 \phi_2(k, \omega, t) - 2\theta) - s_2(k, \omega, t) \sin(2\alpha^2 \phi_2(k, \omega, t) - 2\theta) \right) \\ &+ 2\alpha^2 \left(1 - d_3(k, \omega, t) e^{-2\alpha^2 d_2(k, \omega, t)} e^{-C(t)}\right) + 1. \end{aligned} \quad (3)$$

Here we define $C(t) = 4n_{\text{th}}k^2(1 - \cos \omega t)$ with $n_{\text{th}} = k_B T/(\hbar\omega_M)$ as the classical mean thermal excitation number. Here we have also assumed that α is real.

The existence of quantum revivals in the quantum description can be understood in the following way. The overall behavior of the quantum variance is controlled by the exponentials $\exp[-\alpha^2(1 - \cos 2A(t))]$ and $\exp[-2\alpha^2(1 - \cos A(t))]$. Considering that $\alpha^2 \gg 1$, the two exponentials are nonzero only when the cosine terms are close to 1. To be specific, when $\omega t \approx N\pi/2k^2$ where N is an odd integer, $\exp[-\alpha^2(1 - \cos 2A(t))] \approx 1$ but $\exp[-2\alpha^2(1 - \cos A(t))] \approx 0$. The quantum variance is

approximated as

$$\text{Var}_\theta^{(q)}(t) \approx 2\alpha^2 \cos(2A(t) + \alpha^2 \sin 2A(t) - 2\theta) + 2\alpha^2 + 1, \quad (4)$$

which represents the first quantum revival. When $\omega t \approx N\pi/k^2$ where N is an integer, $\exp[-\alpha^2(1 - \cos 2A(t))] \approx 1$ and $\exp[-2\alpha^2(1 - \cos A(t))] \approx 1$. In this case the quantum variance is approximated as

$$\begin{aligned} \text{Var}_\theta^{(q)}(t) &\approx 2\alpha^2 \left(\cos(2A(t) + \alpha^2 \sin 2A(t) - 2\theta) - \cos(A(t) + \right. \\ &\quad \left. 2\alpha^2 \sin A(t) - 2\theta) \right) + 1, \end{aligned} \quad (5)$$

which, due to the lack of the constant contribution $2\alpha^2$, shows an overall reduction as in the second quantum revival. Note that, for simplicity, we have made the approximations $\exp[-4k^2(1-\cos\omega t)] \approx 1$ and $\exp[-2k^2(1-\cos\omega t)] \approx 1$, which is reasonable as $k^2 \ll 1$.

In contrast, the overall behavior of the classical variance is controlled by $\exp[-\alpha^2 d_1(k, \omega, t)]$ and $\exp[-2\alpha^2 d_2(k, \omega, t)]$. But d_1 and d_2 are close to zero only at the beginning of the interaction. Once $\exp[-\alpha^2 d_1(k, \omega, t)]$ and $\exp[-2\alpha^2 d_2(k, \omega, t)]$ decay to zero, the classical variance stays at $2\alpha^2 + 1$ without further oscillations.

We have considered three semiclassical descriptions based on mean field approximation in the main text. If the oscillator sees only the mean intensity of the field, the variance is

$$\begin{aligned} \text{Var}_\theta^{(sc1)}(t) &= 1 + 2\alpha^2(1 - e^{-C(t)}) \left(1 - \cos(2\alpha^2 A(t) - 2\theta)e^{-C(t)}\right). \end{aligned} \quad (6)$$

If the oscillator sees the energy quanta of the field with field intensity given by a random number following Poisson distribution, the variance becomes

$$\begin{aligned} \text{Var}_\theta^{(sc2)}(t) &= 2\alpha^2 e^{-\alpha^2(1-\cos 2A(t))} e^{-2C(t)} \cos(\alpha^2 \sin 2A(t) - 2\theta) \\ &\quad - 2\alpha^2 e^{-2\alpha^2(1-\cos A(t))} e^{-C(t)} \cos(2\alpha^2 \sin A(t) - 2\theta) \\ &\quad + 2\alpha^2 \left(1 - e^{-C(t)} e^{-2\alpha^2(1-\cos A(t))}\right) + 1. \end{aligned} \quad (7)$$

And if the Poisson distribution is approximated by a Gaussian distribution, the variance turns out to be

$$\begin{aligned} \text{Var}_\theta^{(sc3)}(t) &= 1 + 2\alpha^2(1 - e^{-C(t)} e^{-\alpha^2 A^2(t)}) \\ &\quad \times \left(1 - \cos(2\alpha^2 A(t) - 2\theta)e^{-C(t)} e^{-\alpha^2 A^2(t)}\right). \end{aligned} \quad (8)$$

II. THERMAL INITIAL STATE AND THERMAL BATH FOR THE OSCILLATOR

In the main text we focus on the case where the mechanical oscillator starts from a vacuum state, and it is not subject to thermal noise throughout the evolution. In this section we will analyze the effect of both factors, respectively.

The thermal initial state is well captured by the parameter \tilde{n}_{th} in Eq. (1). A vacuum state corresponds to $\tilde{n}_{\text{th}} = 0$. The initial thermal excitations bring the field variance closer to the constant value $2\alpha^2 + 1$. However, at the end of each mechanical period, the oscillator and the field decouples. At those times the field does not see the thermal noise in the oscillator any more. Fig. 1 shows four examples of how the field variance changes with time, with different thermal initial states of the oscillator. The periodical recombinations of variances with

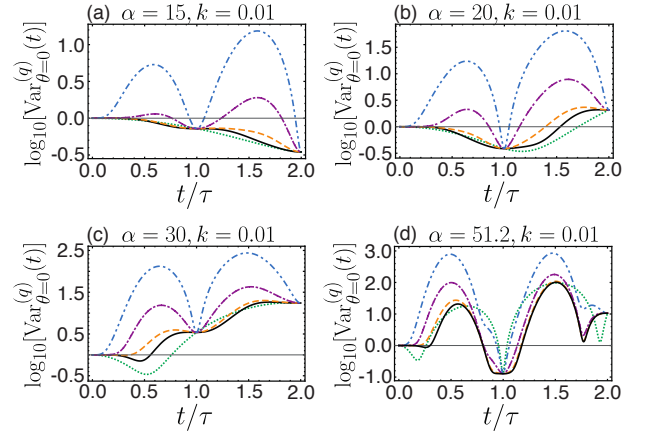


FIG. 1. Variance of the cavity field as a function of time for different combinations of α and k in the quantum picture. Black solid line corresponds to the case where the oscillator starts from the vacuum state. Green dotted line is for the Kerr nonlinear medium that is equivalent to the optomechanical model at the end of each mechanical period. Orange dashed line is for $\tilde{n}_{\text{th}} = 1$ ($T = 2.1$ mK), purple dot-dashed line is for $\tilde{n}_{\text{th}} = 10$ ($T = 15.1$ mK), and blue dot-dot-dashed line is for $\tilde{n}_{\text{th}} = 100$ ($T = 144.8$ mK), where $\omega = 2\pi \times 30$ MHz is assumed.

different initial thermal phonons are clear. The variances at the end of each mechanical period coincide with the case of the equivalent model of Kerr medium as well. Note here we set $\theta = 0$ for simplicity.

Continuous contact of the oscillator with a thermal bath has a different impact on the field variance. In the weak coupling regime, the dynamics is governed by the master equation [1, 2]

$$\begin{aligned} \dot{\rho}(t) &= -i[\hat{H}, \rho(t)]/\hbar + \gamma(\tilde{n} + 1) \left(\hat{b}\rho(t)\hat{b}^\dagger - \frac{1}{2}\hat{b}^\dagger\hat{b}\rho(t) - \frac{1}{2}\rho(t)\hat{b}^\dagger\hat{b} \right) \\ &\quad + \gamma\tilde{n} \left(\hat{b}^\dagger\rho(t)\hat{b} - \frac{1}{2}\hat{b}\hat{b}^\dagger\rho(t) - \frac{1}{2}\rho(t)\hat{b}\hat{b}^\dagger \right), \end{aligned} \quad (9)$$

where \hat{H} is the Hamiltonian

$$\hat{H}/\hbar = \omega\hat{b}^\dagger\hat{b} - \frac{g_0}{\sqrt{2}}\hat{a}^\dagger\hat{a}(\hat{b}^\dagger + \hat{b}), \quad (10)$$

\tilde{n} is the mean phonon number of the bath, and γ characterizes the mechanical decay rate. Fig. 2 shows the numerical result of how the field variance evolves with $\alpha = 2$ and $k = 0.1$ considering computational cost. We assume the oscillator starts from a vacuum state for simplicity, and set $\theta = 0$ for the variance. The variance gradually gets closer to the constant value $2\alpha^2 + 1$. Clearly as zoomed in, the amplitude of quantum revivals is reduced.

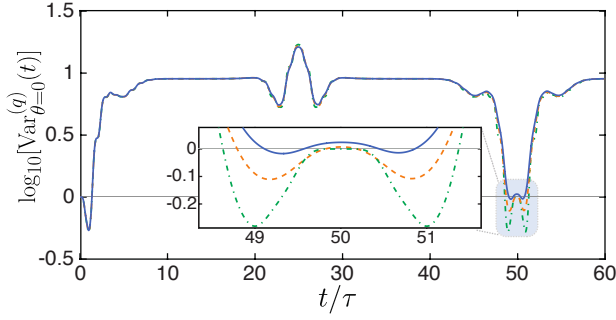


FIG. 2. Variance of the cavity field in the quantum picture as a function of time when the mechanical oscillator is in contact with a thermal bath. $\alpha = 2$, $k = 0.1$. Other parameters are: $\gamma/\omega = 0$, $\tilde{n} = 0$ (green dot-dashed line), $\gamma/\omega = 0.01$, $\tilde{n} = 0$ (orange dashed line), $\gamma/\omega = 0.01$, $\tilde{n} = 0.5$ (blue solid line).

III. DEPENDENCE OF FIELD VARIANCE ON PARAMETERS α AND k

The coherent state amplitude α and interaction strength k both affect how the field variance evolves with time. In this section we take the quantum description as an example to analyze those effects.

As seen from Fig. 1, at the end of each mechanical period, the time derivative of field variance is close to zero, which means the variance does not change rapidly in time. Also the initial thermal phonon excitation does not affect the variance at those times. Considering that the side band resolution ω/κ is usually smaller than 1 or on the order of 1, we choose the variance at $t = \tau$ to represent the amount of squeezing. Usually $\alpha k < 1$ is satisfied. Once we Taylor expand Eq. (1) around $k = 0$, we can see that the product αk directly decides the variance. This is clearly shown in Fig. 3. Especially, the two contours marked in yellow indicate squeezing, and for those two contours $\theta = 0$ is very close to the angle corresponding to the minimum variance.

k itself decides when the quantum revivals appear. As discussed in the main text, they are proportional to $1/k^2$.

IV. DERIVATION OF THE EQUATIONS OF MOTION IN THE FULLY CLASSICAL PICTURE

The physical picture in the classical description is very clear. The mechanical oscillator provides a moving instantaneous boundary to the field, while the field exerts a radiation pressure force on the mechanical oscillator depending on the field intensity [3]. As pointed out in Ref. [4], the field acquires a phase depending on the distance it travels inside the cavity, which is determined by the position of the mechanical oscillator. However, the variance of the field is non-trivially related to both amplitude and phase of the field, which requires a careful analysis. Our starting point is the classical Hamiltonian describing the dynamics of a one-dimensional electromag-

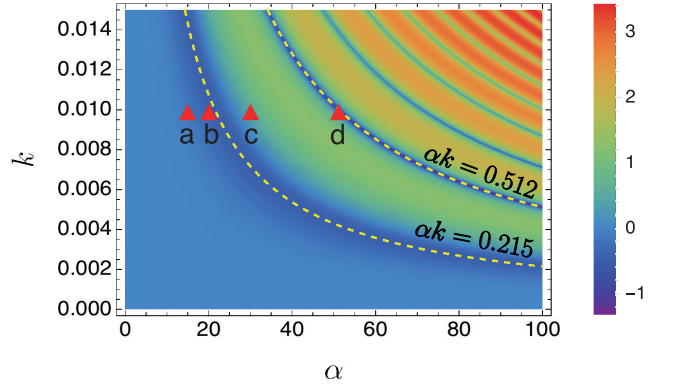


FIG. 3. Variance of the cavity field as a function of the coherent state amplitude α and the rescaled coupling strength k in the quantum picture. Color shows the value of $\log_{10}[\text{Var}_{\theta=0}^{(q)}(t = \tau)]$. Red triangles correspond to the four cases in Fig. 1.

netic field in a cavity with a movable boundary. Especially, the degrees of freedom of the boundary must be included in the overall system's dynamics. The Hamiltonian of the system is found to be [3]

$$\tilde{H} = \frac{p_M^2}{2M} + \frac{1}{2}M\omega^2 x_M^2 + \frac{1}{2}(P_L^2 + \Omega^2 Q_L^2) - \frac{x_M}{L}\Omega^2 Q_L^2, \quad (11)$$

where $\{x_M, p_M\}$ and $\{Q_L, P_L\}$ are pairs of canonical variables for the mechanical oscillator and the field, respectively. To simplify the notations, we rescale the canonical variables as $x = \sqrt{M\omega}x_M$, $p = p_M/\sqrt{M\omega}$, $\tilde{x}_L = \sqrt{\Omega}Q_L$ and $\tilde{p}_L = P_L/\sqrt{\Omega}$. Note that the rescaling keeps the Poisson bracket invariant, so $\{x, p, \tilde{x}_L, \tilde{p}_L\}$ act as canonical variables as well [5]. Now the Hamiltonian becomes

$$\tilde{H} = \frac{1}{2}\omega(x^2 + p^2) + \frac{1}{2}\Omega(\tilde{x}_L^2 + \tilde{p}_L^2) - g_0 x \tilde{x}_L^2. \quad (12)$$

We perform a canonical transformation which maps $\{\tilde{x}_L, \tilde{p}_L\}$ into another pair of canonical variables $\{x_L, p_L\}$ in the frame rotating with frequency Ω , namely

$$\begin{aligned} x_L &= \tilde{x}_L \cos \Omega t - \tilde{p}_L \sin \Omega t, \\ p_L &= \tilde{x}_L \sin \Omega t + \tilde{p}_L \cos \Omega t. \end{aligned} \quad (13)$$

The equations of motion are then found to be

$$\begin{aligned} \frac{dp(t)}{dt} &= -\omega x(t) + g_0 \left(x_L^2(t) \cos^2 \Omega t + p_L^2(t) \sin^2 \Omega t \right. \\ &\quad \left. + x_L(t)p_L(t) \sin 2\Omega t \right), \\ \frac{dx(t)}{dt} &= \omega p(t), \\ \frac{dp_L(t)}{dt} &= g_0 x(t) \left(2x_L(t) \cos^2 \Omega t + p_L(t) \sin 2\Omega t \right), \\ \frac{dx_L(t)}{dt} &= -g_0 x(t) \left(x_L(t) \sin 2\Omega t + 2p_L(t) \sin^2 \Omega t \right). \end{aligned} \quad (14)$$

Note that in Eq. (14) the first order time derivatives of the canonical variables do not depend on $\Omega x(t)$, $\Omega p(t)$, $\Omega x_L(t)$ or $\Omega p_L(t)$, which means that the fast oscillation of the light is already removed by the transformation Eq. (13). The canonical variables evolve on a time scale much slower than the time scale set by the field frequency Ω under usual optomechanical parameters. As a result, we can approximate the equations of motion by taking the time average over the period of the field, which leaves everything unchanged except those related to Ωt , namely, $\cos^2 \Omega t \rightarrow 1/2$, $\sin^2 \Omega t \rightarrow 1/2$ and $\sin \Omega t \cos \Omega t \rightarrow 0$. The effective equations of motion then become

$$\begin{aligned}\frac{dp(t)}{dt} &= -\omega x(t) + \frac{1}{2}g_0(x_L^2(t) + p_L^2(t)), \\ \frac{dx(t)}{dt} &= \omega p(t), \\ \frac{dp_L(t)}{dt} &= g_0 x(t)x_L(t), \\ \frac{dx_L(t)}{dt} &= -g_0 x(t)p_L(t).\end{aligned}\tag{15}$$

It is straightforward to check that Eq. (15) corresponds to the Hamiltonian

$$H = \omega|\beta|^2 - \frac{g_0}{\sqrt{2}}|\alpha_L|^2(\beta^* + \beta),\tag{16}$$

once we define a complex variable describing the field as $\alpha_L = (x_L + ip_L)/\sqrt{2}$ and a complex variable describing

the mechanical oscillator as $\beta = (x + ip)/\sqrt{2}$. Direct comparison with Eq. (10) implies that, $\alpha_L(\beta)$ is the classical version of $\hat{a}(\hat{b})$.

The transformation Eq. (13) together with the average over fast oscillation is essentially the classical counterpart of the rotating wave approximation which is necessary in the derivation of the standard optomechanical Hamiltonian (10), where, in fact, the terms proportional to a^2 and $a^{\dagger 2}$ are neglected [3, 6]. It enables us to solve the equations of motion, Eq. (15), analytically. It is straightforward to check that $\{|\alpha_L|^2, H\} = 0$, where $\{\cdot, \cdot\}$ represents the Poisson bracket. As a result, $|\alpha_L|^2$ is a conserved quantity during the time evolution, as in the quantum case. We can thus directly replace $x_L^2(t) + p_L^2(t)$ with $x_L^2(0) + p_L^2(0)$ in Eq. (15). The solutions of Eq. (15) are then given by

$$\begin{aligned}x(t) &= x(0) \cos \omega t + p(0) \sin \omega t + \frac{g_0}{\omega}|\alpha_L(0)|^2(1 - \cos \omega t), \\ p(t) &= -x(0) \sin \omega t + p(0) \cos \omega t + \frac{g_0}{\omega}|\alpha_L(0)|^2 \sin \omega t, \\ \alpha_L(t) &= \alpha_L(0)e^{ig_0 \int_0^t x(\tau) d\tau} \\ &= \alpha_L(0)e^{iA(t)|\alpha_L(0)|^2} e^{i\frac{g_0}{\omega}(\sin \omega t x(0) + (1 - \cos \omega t)p(0))},\end{aligned}\tag{17}$$

where $x(t)$ ($p(t)$) represents the position (momentum) of the mechanical oscillator, $\alpha_L(t)$ represents the amplitude of the field.

-
- [1] S. Bose, K. Jacobs, and P. Knight, Phys. Rev. A **56**, 4175 (1997).
 - [2] A. Nunnenkamp, K. Børkje, and S. M. Girvin, Phys. Rev. Lett. **107**, 063602 (2011).
 - [3] C. Law, Phys. Rev. A **51**, 2537 (1995).
 - [4] F. Armata, L. Latmiral, I. Pikovski, M. R. Vanner, Č. Brukner, and M. S. Kim, Phys. Rev. A **93**, 063862 (2016).
 - [5] L. N. Hand and J. D. Finch, *Analytical mechanics* (Cambridge University Press, 1998).
 - [6] K. Sala and T. Tufarelli, Sci. Rep. **8**, 9157 (2018).